View metadata, citation and similar papers at core.ac.uk
brought to you by CORE
provided by Apollo

Accurate on-chip measurement of the Seebeck coefficient of high mobility small molecule organic semiconductors

C. N. Warwick, D. Venkateshvaran, and H. Sirringhaus

Citation: APL Mater. **3**, 096104 (2015); doi: 10.1063/1.4931750
View online: http://dx.doi.org/10.1063/1.4931750
View Table of Contents: http://scitation.aip.org/content/aip/journal/aplmater/3/9?ver=pdfcov
Published by the AIP Publishing

Articles you may be interested in

Low-temperature carrier dynamics in high-mobility organic transistors of alkylated dinaphtho-thienothiophene as investigated by electron spin resonance
Appl. Phys. Lett. **105**, 033301 (2014); 10.1063/1.4890962

High mobility n-type organic thin-film transistors deposited at room temperature by supersonic molecular beam deposition
Appl. Phys. Lett. **104**, 143302 (2014); 10.1063/1.4870991

Field-effect modulated Seebeck coefficient measurements in an organic polymer using a microfabricated on-chip architecture
APL Mater. **2**, 032102 (2014); 10.1063/1.4867224

High performance organic field-effect transistors with ultra-thin HfO2 gate insulator deposited directly onto the organic semiconductor
Appl. Phys. Lett. **104**, 013307 (2014); 10.1063/1.4860998

Three-dimensional organic field-effect transistors with high output current and high on-off ratio
Appl. Phys. Lett. **94**, 103307 (2009); 10.1063/1.3098404

APL Photonics is pleased to announce
Benjamin Eggleton as its Editor-in-Chief

This article is copyrighted as indicated in the article. Reuse of AIP content is subject to the terms at: http://aplmaterials.aip.org/about/rights_and_permissions
Downloaded to IP: 131.111.184.102 On: Wed, 11 Nov 2015 14:55:19

APL MATERIALS **3**, 096104 (2015)

Accurate on-chip measurement of the Seebeck coefficient of high mobility small molecule organic semiconductors

C. N. Warwick, D. Venkateshvaran, and H. Sirringhaus
Optoelectronics Group, Cavendish Laboratory, University of Cambridge, J J Thomson Ave., Cambridge CB3 0HE, United Kingdom

(Received 4 August 2015; accepted 14 September 2015; published online 21 September 2015)

We present measurements of the Seebeck coefficient in two high mobility organic small molecules, 2,7-dioctyl[1]benzothieno[3,2-b][1]benzothiophene (C_8-BTBT) and 2,9-didecyl-dinaphtho[2,3-b:2′,3′-f]thieno[3,2-b]thiophene (C_{10}-DNTT). The measurements are performed in a field effect transistor structure with high field effect mobilities of approximately 3 cm^2/Vs. This allows us to observe both the charge concentration and temperature dependence of the Seebeck coefficient. We find a strong logarithmic dependence upon charge concentration and a temperature dependence within the measurement uncertainty. Despite performing the measurements on highly polycrystalline evaporated films, we see an agreement in the Seebeck coefficient with modelled values from Shi *et al.* [Chem. Mater. **26**, 2669 (2014)] at high charge concentrations. We attribute deviations from the model at lower charge concentrations to charge trapping. *© 2015 Author(s). All article content, except where otherwise noted, is licensed under a Creative Commons Attribution 3.0 Unported License.* [http://dx.doi.org/10.1063/1.4931750]

With the measured mobilities of organic semiconductors having increased consistently over the last two decades, organic semiconductors are now not only of interest for applications in field-effect transistors (FETs) but are also being considered as materials for large-area thermoelectrics. Some of the highest reported mobilities have been measured in BTBT and DNTT derivatives.[2–6] A high charge carrier mobility is beneficial for thermoelectric applications as it allows reaching high conductivity values without having to introduce a large carrier concentration that would reduce the Seebeck coefficient. Theoretical calculations by Shi *et al.*[1] show that for pure C_8-BTBT, a high dimensionless thermoelectric figure of merit, ZT, of 0.7 or higher can be expected, where $ZT = \alpha^2\sigma T/\kappa$. Here, α is the Seebeck coefficient, σ is the electrical conductivity, κ is the thermal conductivity, and T is the temperature. This compares with values close to 1 for the commonly used thermoelectric material Bi_2Te_3.[7] Alkylated derivatives such as C_8-BTBT and C_{10}-DNTT are additionally of interest due to their easy solution-processability[2,3,8] and air-stable operation.[9] In this work, we measure for the first time the Seebeck coefficient in both C_8-BTBT and C_{10}-DNTT.

The Seebeck coefficient characterizes the thermoelectric effect and the first order term is simply the ratio of the generated thermo-voltage to applied temperature difference ($\alpha = \Delta V/\Delta T$). The electronic contribution to the Seebeck coefficient has been shown[10] to be equal to

$$\alpha = \frac{k_B}{q}\frac{\int \frac{E-E_F}{k_BT}\sigma(E)dE}{\int \sigma(E)dE}, \tag{1}$$

where E_F is the Fermi level, q is the carrier's charge, and k_B is the Boltzmann constant. For coherent hole-only transport, we can rewrite this as

$$\alpha = \frac{k_B}{e}\left(\frac{E_F - E_V}{k_BT} + A_V\right), \tag{2}$$

where E_V is the valence band edge and A_V is the heat of transport constant defined from Equation (1). A_V represents the difference between a conductivity-weighted average energy and the valence band edge, and is not generally a constant, but is 1 when $\sigma(E)$ is constant above E_V

 ©Author(s) 2015

This article is copyrighted as indicated in the article. Reuse of AIP content is subject to the terms at: http://aplmaterials.aip.org/about/rights_and_permissions Downloaded to IP: 131.111.184.102 On: Wed, 11 Nov 2015 14:55:19

and takes higher values if $\sigma(E)$ increases above E_V. Measurements of the temperature dependence of the field effect mobility[4] and first principles calculations of the transport in C_8-BTBT[1,11] both support a band-like, rather than a hopping, transport mechanism as being dominant in these materials, corresponding to $\sigma(E)$ changing more slowly above E_V. We therefore expect A_V to be low. Furthermore, for the relatively low charge carrier concentrations in typical FETs, $E_F - E_V \gg k_B T$, and hence, the first term in Equation (2) will be dominant. At these concentrations, the distribution of charges is approximately Boltzmann-like, the hole concentration, n, then being equal to

$$n = N_{\text{eff}} \exp\left(-\frac{E_F - E_V}{k_B T}\right) \approx N_{\text{eff}} \exp\left[-\left(\frac{e}{k_B}\right)\alpha\right], \tag{3}$$

where N_{eff} is the effective density of states and we have substituted in Equation (2) (ignoring A_V) to get the second expression. From this, we see that the Seebeck coefficient is expected to be logarithmically dependent on charge concentration and independent of temperature (for a given charge concentration). The assumptions made here are appropriate for the modelling performed in Shi *et al.*,[1] which we compare our measurements to. They calculate the Seebeck coefficient from first principles electronic structure calculations in conjunction with Boltzmann transport theory.

In addition to the electronic contribution to the Seebeck coefficient, there is also a contribution from carrier induced vibrational softening of molecular motions, arising from electron-phonon coupling. However, this is expected to be independent of charge concentration.[12] Therefore, we expect the measured Seebeck coefficient to exhibit the charge concentration dependence found from rearranging Equation (3). Any temperature dependence will be sensitive to deviations from this model. By measuring the Seebeck coefficient in a FET structure, we are able to modulate the charge concentration (through modulation of the gate voltage) and the temperature dependence independently. This is in contrast to doping studies where the level of doping (and hence the charge concentration) will be dependent upon temperature.

Following on from previous work,[13,14] we integrate an on-chip heater with a FET structure (Figure 1(a)) and use the FET source and drain as temperature sensors. These modifications are in

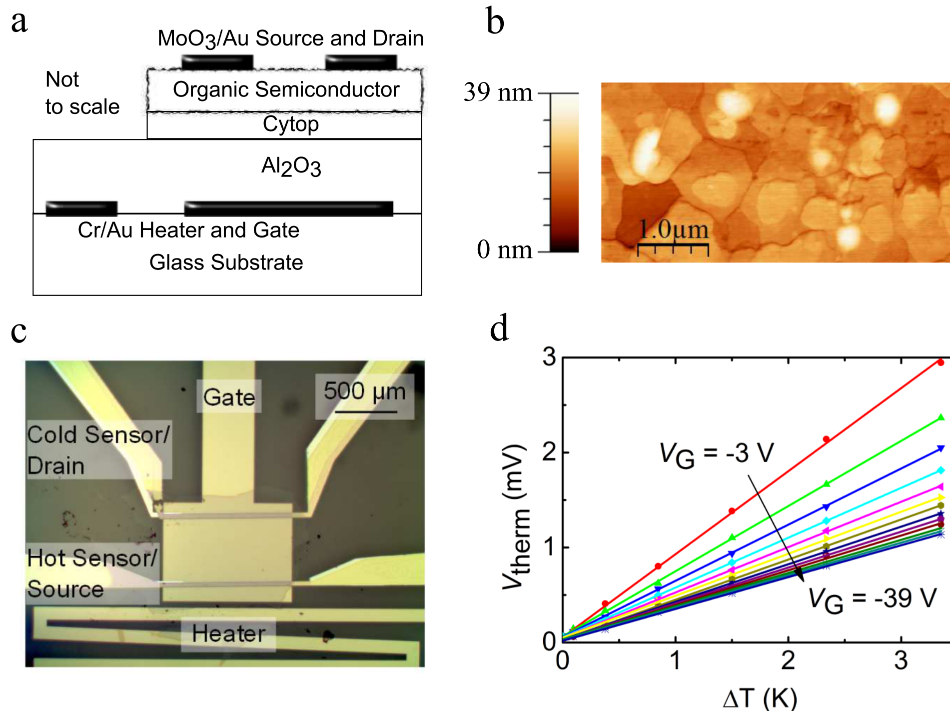

FIG. 1. (a) A schematic diagram of the device architecture, (b) an AFM image of the surface of the evaporated film, (c) an optical micrograph of a working device, and (d) the measured thermal voltage for different gate voltages.

This article is copyrighted as indicated in the article. Reuse of AIP content is subject to the terms at: http://aplmaterials.aip.org/about/rights_and_permissions
Downloaded to IP: 131.111.184.102 On: Wed, 11 Nov 2015 14:55:19

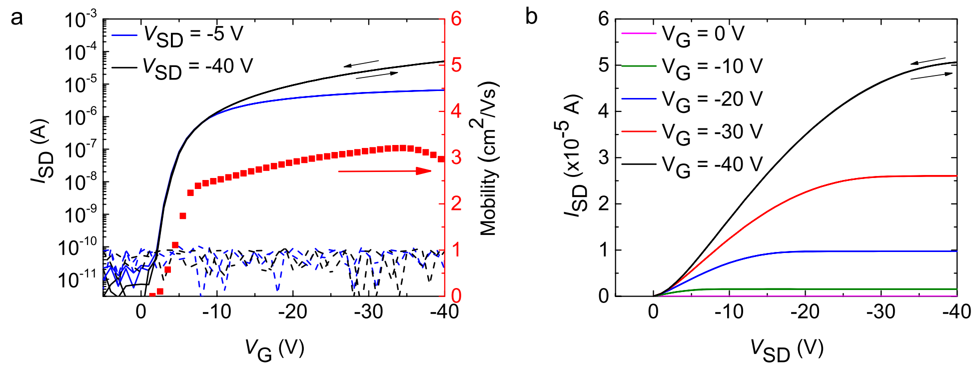

FIG. 2. (a) Typical transfer curves in the linear and saturation regime plotted with field effect mobility (at $V_{SD} = -40$ V). The dashed lines show the gate leakage. (b) Output curves for the same device.

contrast to Seebeck measurements reported elsewhere that tend to use an external heater or Peltier elements and extrapolate the temperature difference from sensors outside the active area.[15–18] Our on-chip measurement configuration minimizes errors and inconsistencies associated with voltage and temperature probe misalignment.[19] The architecture of our device has been inverted from the previous work to feature a bottom gate with top contacts, as this was necessary to achieve efficient charge injection for these materials.

The gate and heater consist of evaporated films of Cr (2 nm) and Au (25 nm) patterned by photolithography. We use a bi-layer dielectric of 200 nm atomic layer deposited Al_2O_3 and 70 nm spincoated Cytop (an amorphous fluorinated polymer). Using two dielectric layers allows us to consistently fabricate devices with very low gate leakage, often at the detection limit of the semiconductor parameter analyzer, even at low source-drain voltages (Figure 2(a)). This is important because the floating potential at the drain may easily be perturbed from the true thermo-voltage by the potential at the gate, if the dielectric is insufficiently resistive. Having the lower k dielectric Cytop (k = 2.1) at the interface with the organic semiconductor also reduces the amount of disorder at the interface,[20,21] giving a near-constant gate-dependence of the field effect mobility at approximately 3 cm^2/Vs, and no hysteresis in the transfer curves (Figure 2).

The C_8-BTBT or C_{10}-DNTT (50 nm) is evaporated through a foil shadow mask and any excess semiconductor outside the active area is scratched away. This is to avoid contributions to the thermo-voltage from outside the active area, which can cause the Seebeck coefficient to be overestimated.[22] The crystalline domains are observed using Atomic Force Microscopy (AFM) to be up to 1 μm in diameter (Figure 1(b)). Top contacts are evaporated through a shadow mask (7 nm of MoO_3 and 25 nm of Au). On the parts of the top contact pattern outside of the active area, an additional much thicker layer of metal is evaporated to ensure that the resistance of the sensors is dominated by the resistance in the active area—this is needed to accurately derive the temperature difference across the channel. A simple calculation integrating a linear temperature gradient over the geometry of the sensors gives an error of 4% for the cold sensor temperature and negligible for the hot sensors. The difference in error arises from the fact that the cold sensor extends much further from the channel than the hot sensor and thus experiences a larger temperature gradient across it. The temperature gradient is expected to decay faster than linearly, which would result in smaller errors. Devices were made with a range of channel lengths: 100, 200, and 500 μm with a channel width of 1 mm and a sensor width of 35 μm.

To measure the temperature difference across the two sensors, two calibration procedures are required. First, the resistances of the two sensors are measured at different cryostat temperatures and used to calculate their temperature coefficient of resistance (TCR). Then, the resistance of the two sensors is measured while sweeping the heater power. The calculated TCR can then be used to derive the temperature difference at each heater power. Typically, the cold sensor is raised by ~3 K, and the hot sensor by ~6 K in a device with a channel length of 500 μm. The thermo-voltage is measured while sweeping the heater power and the gate voltage. Each Seebeck coefficient can

This article is copyrighted as indicated in the article. Reuse of AIP content is subject to the terms at: http://aplmaterials.aip.org/about/rights_and_permissions Downloaded to IP: 131.111.184.102 On: Wed, 11 Nov 2015 14:55:19

then be calculated from a fit to the thermo-voltage at multiple heater powers—typically 7 points are taken (Figure 1(d)). All measurements are performed in high vacuum.

The errors in the Seebeck values are conservatively estimated. The aforementioned contribution from the non-zero resistance of the sensors outside the active area is added to a number of other contributions. First, from the drift of the sample temperature from the cryostat temperature at low temperatures (taken to be up to 1 K different over a 100 K range). Second, an assumed error of the order of the ratio of the sensor width to the channel length and third, a contribution from the errors associated with the fitting procedures (this is in fact the smallest contribution). An example of the final fit required to extract the Seebeck coefficient is shown in Figure 1(d).

To compare devices, we plot the Seebeck coefficient against the charge density, n, calculated from $n = C(V_{\text{Gate}} - V_{\text{Accum}})/t_{\text{Accum}}$. The capacitance per area, C, we measure for each device against gate voltage and the accumulation voltage, V_{Accum}, is the onset of accumulation extracted from the C-V measurements. The thickness of the accumulation layer, t_{Accum}, is taken to be the thickness of one monolayer (29.18 Å for C_8-BTBT).

We showcase two C_8-BTBT devices' temperature dependent Seebeck values (Figures 3(a) and 3(b)). The Seebeck coefficient is positive, consistent with hole transport. Even at high gate voltages, the Seebeck coefficient is much greater than k_B/e ($\approx$86 μV/K), implying that the Fermi level remains firmly in the band gap throughout. The Seebeck values decrease approximately logarithmically with charge concentration, as expected. The expected charge carrier concentration dependence has not always been observed in the literature of Seebeck measurements in molecular semiconductors.[16,23]

The absolute value of the Seebeck coefficient is close to that calculated by Shi *et al.*[1] at high gate voltages but rises more steeply at lower gate voltages, as can be seen in Figure 3(c). As their model assumes a perfect crystalline structure whereas our own measurements are performed on highly polycrystalline evaporated films, we suggest that this difference is due to the presence of trap states within the band gap of the semiconductor. Trap states tend to have the effect of pinning the Fermi level to states within the band gap and are particularly effective in doing so at low charge concentrations. The difference between E_F and E_V (and therefore the Seebeck coefficient) is thereby increased at lower charge concentrations. An alternative way of expressing this is that the *mobile* hole concentration that contributes is lower in the experiment than it would be in the absence of traps, and this increases the Seebeck coefficient in a regime where the Seebeck coefficient is dominated by the entropy of mixing associated with adding a carrier into the valence band density of states.

As the charge concentration increases, the Seebeck values approach those theoretically predicted by Shi *et al.* and the gradient $\partial\alpha/\partial ln(n)$ tends to the computed value. We interpret this to mean that at high gate voltages, the majority of charges are not trapped due to the trap states having been largely filled. The variation in gradient across all gate voltages has not been observed in previous work on a number of polymers,[14] and to the authors' knowledge has not been clearly observed in other organic semiconductors. A more quantitative analysis of the observed variation of Seebeck coefficient with gate voltage in terms of the density of states of the semiconductor within the band gap is underway and will be reported elsewhere.

As Shi *et al.*[1] do not model contributions to the Seebeck coefficient from carrier induced vibrational softening, the agreement of our experimental data with the theory at high charge concentrations suggests that any vibrational contributions to the Seebeck effect may be relatively small. The difference between the measured and theoretical Seebeck values at the highest charge concentrations at 300 K is approximately 60 μV/K with an error of 40 μV/K suggesting that any vibrational contribution if present would have to be less than 100 μV/K.

The measured Seebeck values are nearly temperature independent, the change with temperature being a similar magnitude to the error bars. However, a slight decrease with decreasing temperature is consistently measured in all samples. As the error bars are relatively small, they bound the temperature dependence to a limited range. A strong temperature dependence of the Seebeck coefficient arises when charges are distributed within a disorder broadened density of states, such that the difference between E_F and E_V does not vary linearly with temperature, or if the charge carrier

This article is copyrighted as indicated in the article. Reuse of AIP content is subject to the terms at: http://aplmaterials.aip.org/about/rights_and_permissions
Downloaded to IP: 131.111.184.102 On: Wed, 11 Nov 2015 14:55:19

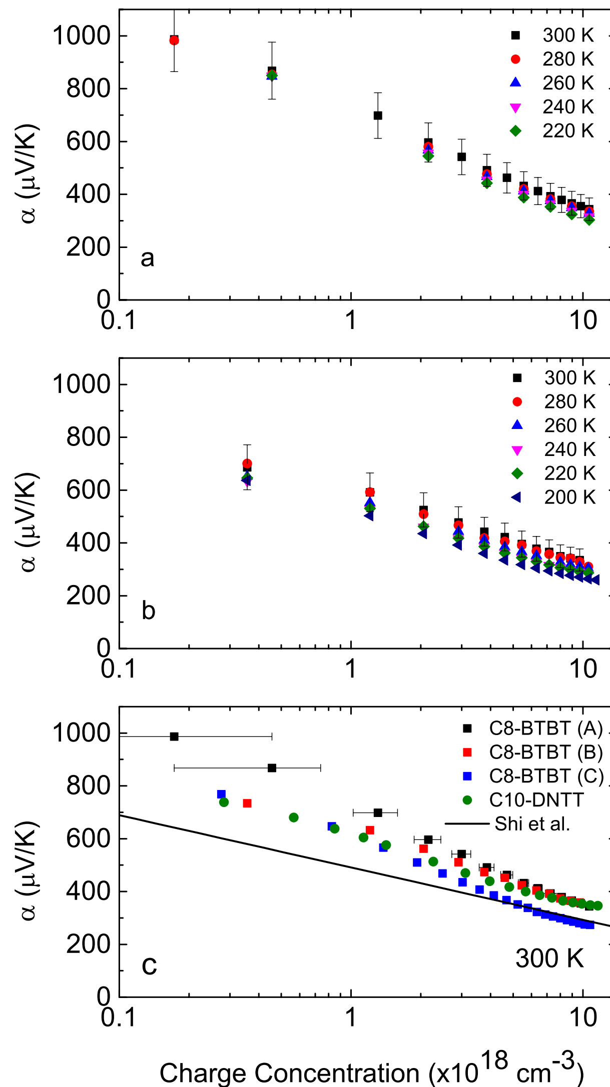

FIG. 3. ((a) and (b)) Seebeck values at different temperatures and gate voltages for two C_8-BTBT devices with a 500 μm channel length. The temperatures are those of the cold finger of the cryostat. (c) Multiple devices at 300 K compared to computed values in Ref. 1. The horizontal error bars represent an uncertainty of 1 V in the onset of accumulation. Both vertical and horizontal error bars apply to all points, but the vertical error bars are just included for 300 K in (a) and (b) and the horizontal just for one device in (c) for clarity.

mobility varies strongly with energy across the density of states, such that the heat of transport constant will become temperature dependent. Our measured temperature invariance therefore suggests that the charges occupy a narrow distribution of energies. In BTBT, there are good reasons to assume the transport mechanism to be band-like, as we have already discussed. We therefore suggest that absence of a significant temperature dependence of the Seebeck coefficient reflects a narrow energetic distribution of hole carriers above the valence band edge. When the trap density of states is shallow and the density of states in the band is high, the Fermi level remains far below the band edge and the carrier distribution is dominated by states at the edge of the valence band, even though the valence band itself may be wider than k_BT. This picture is supported by the agreement to the modelling in Shi *et al.*[1] at high charge concentrations. We note that a similar temperature invariance is measured in single crystalline Rubrene[15]—a material for which band-like transport is even better established. Temperature independent Seebeck measurements have also recently been reported by our group on a series of high mobility conjugated polymers,[14] although there are detailed differences in the magnitude and carrier concentration dependence of the Seebeck coefficient between

This article is copyrighted as indicated in the article. Reuse of AIP content is subject to the terms at: http://aplmaterials.aip.org/about/rights_and_permissions Downloaded to IP: 131.111.184.102 On: Wed, 11 Nov 2015 14:55:19

these two systems that will not be discussed further here. Although the band transport physics of highly crystalline molecular semiconductors is clearly different from that of high mobility conjugated polymers, the common feature between the two systems that is responsible for the large and near-temperature independent Seebeck coefficient is that the energetic disorder in both systems is sufficiently low that the Fermi level resides far below the conducting states in a region of the density of states in which it is not pinned by a broad localized tail state distribution.

The Seebeck values are consistent across multiple devices (Figure 3(c)). We also plot values measured for a C_{10}-DNTT device. They fall within the range reported for C_8-BTBT, and in all cases feature only a weak temperature dependence close to the experimental measurement error. C_{10}-DNTT is structurally similar to C_8-BTBT in its herring-bone packing motif, and these measurements confirm that the density of states for both is correspondingly similar.

We can estimate a ZT value for the accumulation layer in our thin films, taking κ equal to 0.18 W/Km, as derived in Ref. 1. We find ZT is at its greatest for the highest measured charge concentrations, reaching approximately 0.04 at 300 K. This is compared to a theoretical value of approximately 0.6 at these charge concentrations. This discrepancy can be entirely explained by our measured device mobilities being an order of magnitude lower than what was assumed in the theoretical calculation. This should only be considered as a rough guideline as for a more meaningful and accurate estimate of ZT measurements on bulk doped samples need to be performed of course.

In conclusion, we have measured the Seebeck values for C_8-BTBT and C_{10}-DNTT. The observed magnitude of the Seebeck coefficient and its dependency on charge concentration and temperature are consistent with theoretical predictions. The convergence to modelled Seebeck values, decreasing slope $\partial\alpha/\partial ln(n)$, and limited temperature dependence (bound by the measurement errors) all suggest that the trapped states are few and shallow enough that they may be largely filled within the range of charge concentrations measured. Our experimental study confirms that with further improvements in mobility, high mobility molecular semiconductors such as BTBT and DNTT are attractive materials for thermoelectric devices.

The authors would like to thank David Emin for discussions and Nippon Kayaku for providing the organic semiconductors. We gratefully acknowledge funding from the Engineering and Physical Sciences Research Council (EPSRC).

[1] W. Shi, J. Chen, J. Xi, D. Wang, and Z. Shuai, Chem. Mater. **26**, 2669 (2014).
[2] H. Minemawari, T. Yamada, H. Matsui, J. Tsutsumi, S. Haas, R. Chiba, R. Kumai, and T. Hasegawa, Nature **475**, 364 (2011).
[3] K. Nakayama, Y. Hirose, J. Soeda, M. Yoshizumi, T. Uemura, M. Uno, W. Li, M. J. Kang, M. Yamagishi, Y. Okada, E. Miyazaki, Y. Nakazawa, A. Nakao, K. Takimiya, and J. Takeya, Adv. Mater. **23**, 1626 (2011).
[4] C. Liu, T. Minari, X. Lu, A. Kumatani, and K. Takimiya, Adv. Mater. **23**, 523 (2011).
[5] K. Takimiya, H. Ebata, K. Sakamoto, T. Izawa, T. Otsubo, and Y. Kunugi, J. Am. Chem. Soc. **128**, 12604 (2006).
[6] U. Zschieschang, M. J. Kang, K. Takimiya, T. Sekitani, T. Someya, T. W. Canzler, A. Werner, J. Blochwitz-Nimoth, and H. Klauk, J. Mater. Chem. **22**, 4273 (2012).
[7] G. S. Nolas, J. Sharp, and J. Goldsmid, *Thermoelectrics: Basic Principles and New Materials Developments* (Springer Science & Business Media, 2013), Vol. 45.
[8] T. Uemura, Y. Hirose, M. Uno, K. Takimiya, and J. Takeya, Appl. Phys. Express **2**, 111501 (2009).
[9] H. Ebata, T. Izawa, E. Miyazaki, K. Takimiya, M. Ikeda, H. Kuwabara, and T. Yui, J. Am. Chem. Soc. **129**, 15732 (2007).
[10] H. Fritzsche, Solid State Commun. **9**, 1813 (1971).
[11] H. Kobayashi, N. Kobayashi, S. Hosoi, N. Koshitani, D. Murakami, R. Shirasawa, Y. Kudo, D. Hobara, Y. Tokita, and M. Itabashi, J. Chem. Phys. **139**, 014707 (2013).
[12] D. Emin, Phys. Rev. B **59**, 6205 (1999).
[13] D. Venkateshvaran, a. J. Kronemeijer, J. Moriarty, D. Emin, and H. Sirringhaus, APL Mater. **2**, 032102 (2014).
[14] D. Venkateshvaran, M. Nikolka, A. Sadhanala, V. Lemaur, M. Zelazny, M. Kepa, M. Hurhangee, A. J. Kronemeijer, V. Pecunia, I. Nasrallah, I. Romanov, K. Broch, I. McCulloch, D. Emin, Y. Olivier, J. Cornil, D. Beljonne, and H. Sirringhaus, Nature **514**, 384 (2014).
[15] K. P. Pernstich, B. Rössner, and B. Batlogg, Nat. Mater. **7**, 321 (2008).
[16] A. von Mühlenen, N. Errien, M. Schaer, M.-N. Bussac, and L. Zuppiroli, Phys. Rev. B **75**, 115338 (2007).
[17] O. Bubnova, M. Berggren, and X. Crispin, J. Am. Chem. Soc. **134**, 16456 (2012).
[18] Y. Xuan, X. Liu, S. Desbief, P. Leclère, M. Fahlman, R. Lazzaroni, M. Berggren, J. Cornil, D. Emin, and X. Crispin, Phys. Rev. B **82**, 1 (2010).
[19] J. Martin, J. Electron. Mater. **42**, 1358 (2012).
[20] J. Veres, S. Ogier, and G. Lloyd, Chem. Mater. **16**, 4543 (2004).
[21] I. N. Hulea, S. Fratini, H. Xie, C. L. Mulder, N. N. Iossad, G. Rastelli, S. Ciuchi, and a. F. Morpurgo, Nat. Mater. **5**, 982 (2006).
[22] S. V. Reenen and M. Kemerink, Org. Electron. **15**, 2250 (2014).
[23] W. C. Germs, K. Guo, R. a. J. Janssen, and M. Kemerink, Phys. Rev. Lett. **109**, 016601 (2012).

This article is copyrighted as indicated in the article. Reuse of AIP content is subject to the terms at: http://aplmaterials.aip.org/about/rights_and_permissions Downloaded to IP: 131.111.184.102 On: Wed, 11 Nov 2015 14:55:19